JOURNAL OF MATERIALS SCIENCE 32 (1997) 5797–5804

Computer simulation of A2/B2 second-order phase transition based upon the Khachaturyan diffusion equation

A. M. MEBED, T. KOYAMA, T. MIYAZAKI
Department of Materials Science and Engineering, Nagoya Institute of Technology, Nagoya 466, Japan

A computer simulation, based on the Khachaturyan diffusion equation, is presented to develop the kinetics of the morphological evolution of the A2/B2 second-order phase transition in a binary solid solution. The evolution of the occupation probability, as a function of composition, shows a good similarity to the actual micrographs experimentally obtained based on the macroscopic composition gradient method. These results are used in parallel with the results of the evolution of the long-range order parameter as a function of the ageing time, to verify a new concept of the ordering behaviour inside the ordered phase.

1. Introduction

Since the idea of the order–disorder phenomenon in a solid solution was proposed by Tamman [1] in 1919, it has attracted much attention from physicists as well as metallurgists. It is known that if the temperature variation is in a range entirely below the critical ordering temperature, a substantial number of alloys are ordered, while if it is entirely above the critical temperature, the alloy is disordered. By ordering, the lattice sites can be grouped into sublattices, each of which is occupied predominately by one kind of atom. In the disordered state, no such grouping is possible, i.e. each sublattice is occupied by the various constituents at random [2]. When the alloy is ordered, a non-zero correlation exists between the kind of atom on a given site and that on a distant site, the measure of this being the "long-range order parameter". In a disordered alloy, a correlation, called the "short-range order parameter", still exists between the kinds of atoms at sites close to each other. Thus, by controlling the long-range and short-range order parameters, the processing of technologically advanced materials can be controlled.

From this point of view, many works have dealt with this phenomenon, some experimentally, some thermodynamically and yet others theoretically. While the thermodynamic approach allows close examination of the possibility of the appearance of the metastable phase, as well as the phase-stability limits under given thermodynamic conditions on the phase diagram (in this field and especially for the second kind of ordering, see, for example, the work of Allen and Cahn [3], Kubo and Wayman [4], Semenovsakya [5] and Soffa and Laughlin [6]), the values of such properties are strictly independent of the path by which the equilibrium state is approached. This leads to the requirement of a kinetics model, and consequently, various models have been proposed, such as the chemical reaction-rate equation [7], the Markovian-type stochastic equation [8], the master equation approach [9], the Chan–Hilliard-type kinetic equation [10], the path probability method (PPM) [11, 12], and others.

The kinetics of the disorder → order transition in binary alloy, was recently studied by Fultz [13] using Mote Carlo simulation and the path probability method, by Chen and Simmons [14] by the cluster activation method, and by Sato and co-workers [11, 12] by the vacancy mechanism of atomic migration using the path probability method of time-dependent cooperative phenomena, and choosing the pair approximation. An experimental study of the thermodynamic behaviour of the domain walls when approaching the order–disorder transition from below, was performed by Loiseau *et al.* [15].

We were interested in studying this process theoretically, according to the Onsager-type diffusion equation (developed by Khachaturyan and thus called the Khachaturyan equation) with the concentration wave formalism [16] to describe the kinetics of a second-order phase transition from the A2 disordered phase going through the B2 ordered phase. The validity of the application of that equation to describe this process with all its characterizing features and investigation of the temporal structural transformation of the morphological evolution during diffusion-phase transition in the binary solid solution were also studied.

2. Calculation method

The analytical approach and definition of terms were developed previously [17–19]; brief details are given because it is just a tool to approach our goal.

0022–2461 © *1997 Chapman & Hall*

The kinetic equation used for calculating the phase transformation is the phenomonological Onsager's equation. In this equation, the time evolution the rate of occupation probability, $n(\mathbf{p}, t)$, for solute atoms to be at a crystal lattice site, $\mathbf{p}$, at time, t, is proprtional to the thermodynamics driving force, is given by

$$\frac{\mathrm{d}n(\mathbf{p}, t)}{\mathrm{d}t} = \sum_{\mathbf{p}'} \frac{L(\mathbf{p} - \mathbf{p}')c(1-c)}{RT}\left[\frac{\delta F}{\delta n(\mathbf{p}', t)}\right] \quad (1)$$

where $L(\mathbf{p} - \mathbf{p}')$ is a matrix of kinetic coefficients which represents the diffusion from site $\mathbf{p}$ to $\mathbf{p}'$ during unit time, R is the gas constant, T is the temperature, and c is the solute atom composition. The internal energy, F, is represented by the phenomenological expression

$$\begin{aligned} F = \frac{1}{2}\sum_{\mathbf{p}'}\sum_{\mathbf{p}''} W[\mathbf{p}' - \mathbf{p}'', T]\, n(\mathbf{p}')n(\mathbf{p}'') \\ + K_{\mathrm{B}}T\sum_{\mathbf{p}'}\{n(\mathbf{p}')\ln n(\mathbf{p}') \\ + [1 - n(\mathbf{p}')]\ln[1 - n(\mathbf{p}')]\} \end{aligned} \quad (2)$$

where $\mathbf{p}$ is a position vector, $W[\mathbf{p}' - \mathbf{p}'', T]$ is the interaction energy between atoms at interatomic distance $(\mathbf{p}' - \mathbf{p}'')$.

Substituting the derivative of Equation 2 into Equation 1, followed by Fourier transformation, gives

$$\begin{aligned} \frac{\mathrm{d}\tilde{n}(k, t)}{\mathrm{d}t} = \frac{c(1-c)}{RT}\widetilde{L(k)} \\ \times\left(V(k)\tilde{n}(k) + RT\left\{\ln\left[\frac{n(\mathbf{p}', t)}{1 - n(\mathbf{p}', t)}\right]\right\}_{\mathrm{F}}\right) \end{aligned} \quad (3)$$

where

$\left\{\ln\left[\frac{n(\mathbf{p}', t)}{1 - n(\mathbf{p}', t)}\right]\right\}_{\mathrm{F}}$ is the Fourier transform of

$$\left\{\ln\left[\frac{n(\mathbf{p}', t)}{1 - n(\mathbf{p}', t)}\right]\right\} \quad (4)$$

$$\tilde{n}(k) = 1/N^3\sum_{\mathbf{p}''} n(\mathbf{p}'')\exp(-ik\beta\mathbf{p}'') \quad (5)$$

$$V(k) = \sum_{\mathbf{p}' - \mathbf{p}''} W(\mathbf{p}' - \mathbf{p}'', T)\exp[-ik\beta(\mathbf{p}' - \mathbf{p}'')] \quad (6)$$

$$\widetilde{L(k)} = \sum_{\mathbf{p} - \mathbf{p}'} L(\mathbf{p} - \mathbf{p}')\exp[-ik\beta(\mathbf{p} - \mathbf{p}')] \quad (7)$$

k is a wave number of the Fourier wave, N is the maximum number of k, $\beta = 2\pi/L$ where L is the length of the calculation region.

The concentration wave formalism for the second-phase transformation is

$$\begin{aligned} n(\mathbf{p}) &= c + c\eta\exp(ik\beta\mathbf{p}) \\ &= c + c\eta\cos[\pi(m + n)] \end{aligned} \quad (8)$$

Substituting Equation 8 into Equation 2 gives an expression for F as a function of c, T and η. Minimizing it with respect to η taking into consideration that $\eta \to 0$ at the disordered phase, we can obtain the phase diagram of the order–disorder transition line represented in Fig. 1.

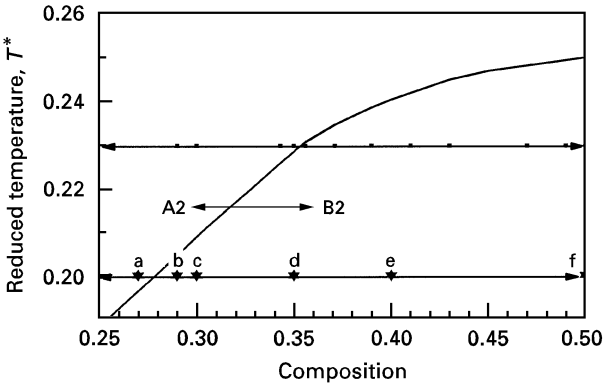

Figure 1 The stable order–disorder transition line of the second kind; (■) calculation points at $T^* = 0.23$, (★) simulation points at $T^* = 0.2$ for Fig. 3.

The initial disordered distribution of the solute atoms is described by an occupation probability profile, $(\mathbf{p}, t)$, with a very small random number. The progress of $c(\mathbf{p}, t)$ with ageing time can be obtained by using the Euler technique

$$\tilde{n}(k, t + \Delta t) = \tilde{n}(k, t) + [\partial\tilde{n}(k, t)/\partial t]\Delta t \quad (9)$$

3. Simulation technique

To describe the kinetics of ordering, the model of the nearest neighbour may be ambiguous, and it is necessary to consider the higher neighbour interactions [20].

A binary alloy on a two-dimensional square lattice with first, second and third-neighbour pairwise interactions is used, where the interchange energies are selected as $w_1 = 1.0$, $w_2 = -0.8$, $w_3 = -0.6$. The interchange energies are arbitrarily chosen with the only requirement that they produce a two-phase field of ordered and disordered phases [21].

By using the kinetics coefficients of elementary diffusional jumps to the nearest and the next-nearest neighbours sites – this selection makes it act as a snapshot, with a feature characterizing the second-order phase, as is shown later – $\widetilde{L(k)}$ can be expressed as

$$\begin{aligned} \widetilde{L(k)}_0 &= -\sum_{\mathbf{p} - \mathbf{p}'}^{*} L(\mathbf{p} - \mathbf{p}')\{1 - \exp[-ik\beta(\mathbf{p} - \mathbf{p}')]\} \\ &= -4L_1(2 - \cos^2\pi h - \cos^2\pi l) \\ &\quad - 8L_2(2\cos^2\pi h\cos^2\pi l - \cos^2\pi h - \cos^2\pi l) \end{aligned} \quad (10)$$

because it is taken into consideration that

$$\sum_{\mathbf{p} - \mathbf{p}'} L(\mathbf{p} - \mathbf{p}') = 0 \quad (11)$$

where the definition and the value of L_1 and L_2 are the same as those selected by Wang *et al.* [22].

4. Results and discussion

4.1. Snapshot

To test the snapshot property of Khachaturyan's equation, we made the initial condition of the occupation probability close to 0 or 1, only. Accordingly, its

time development produces the results represented in Fig. 2. At $t^* = 0.0$ (Fig. 2a), a completely disordered state exists, with the existence of a short-range order clearly apparent in the figure. At $t^* = 0.1$ (Fig. 2b), the cooperative phenomenon occurs where the formation of the ordered domains characterizes the presence of the second–order phase. With increasing ageing time (Fig. 2c, $t^* = 0.3$), coarsening of the antiphase domains occurs and the domains come close to each other, followed by a coalescence process giving larger ordered domains. At this point the ordering process is completed, as shown in Fig. 2d, $t^* = 1.0$. The total area now consists of ordered domains with antiphase boundaries (APBs), but the APBs still have a high curvature. For example, if we follow a particle of circular shape in Fig. 2d, we find that it does not shrink because of the increase in the free energy of the system, but it moves closer to other APBs, making contact at some point. This causes the circle to break and open at this point, as shown in Fig. 2e, $t^* = 1.6$. With increasing ageing time, a simple movement of APBs, which have a high curvature, occurs for further reduction in the energy of the system (Fig. 2f, $t^* = 2.2$).

4.2. The competition of ordering with the composition

Because the disordered state is quenched below the ordering transition temperature, we expect ordering to occur, but how does the kinetic of ordering behave as a function of composition?

Fig. 3 shows our simulation at a reduced temperature ($T^* = 0.2$) with the same ageing time for the computational cell 128×128. The different grey levels represent values of the function $n(\mathbf{p})$ at each lattice site, a completely black square represents $n(\mathbf{p})$ close to 1, and a completely white one possible $n(\mathbf{p})$ close to 0.

The first point is represented by point "a" on the phase diagram (Fig. 1) where the composition $c = 0.27$ just outside the ordering line. This represents a completely disordered state with an occupation probability $n(\mathbf{p}) = c + \delta$ where δ is a random noise between -0.002 and 0.002, i.e. it is close to the average composition, with $\eta = 0.0$, Fig. 3a.

Fig. 3b represents the simulation of point "b" inside the ordered phase and close to the transition line ($c = 0.29$) on the reduced phase diagram. It clearly shows that the configuration consists of ordered domains with a small area at the centre having a high LRO parameter surrounded also by an ordered area with a gradient LRO parameter. On going away from the centre, the LRO parameters become smaller, vanishing at the edge of the domains to form the APBs which have a thickness slightly larger than that for the stoichiometry and is also shorter.

With a small increase of concentration ($c = 0.3$, point "c", Fig. 3c) the ordered domains become close to each other, making the thickness of the APBs smaller than that of the former case, and approximately the same as the stoichiometry. In addition, the ordered area, which has a high LRO parameter, increase, causing the area of the gradient value of LRO parameter to decrease. At $c = 0.35$ (point d, Fig. 3d), the thickness of the APBs is the same as for the stoichiometry and the value of the LRO parameter becomes zero more sharply and thus makes all the

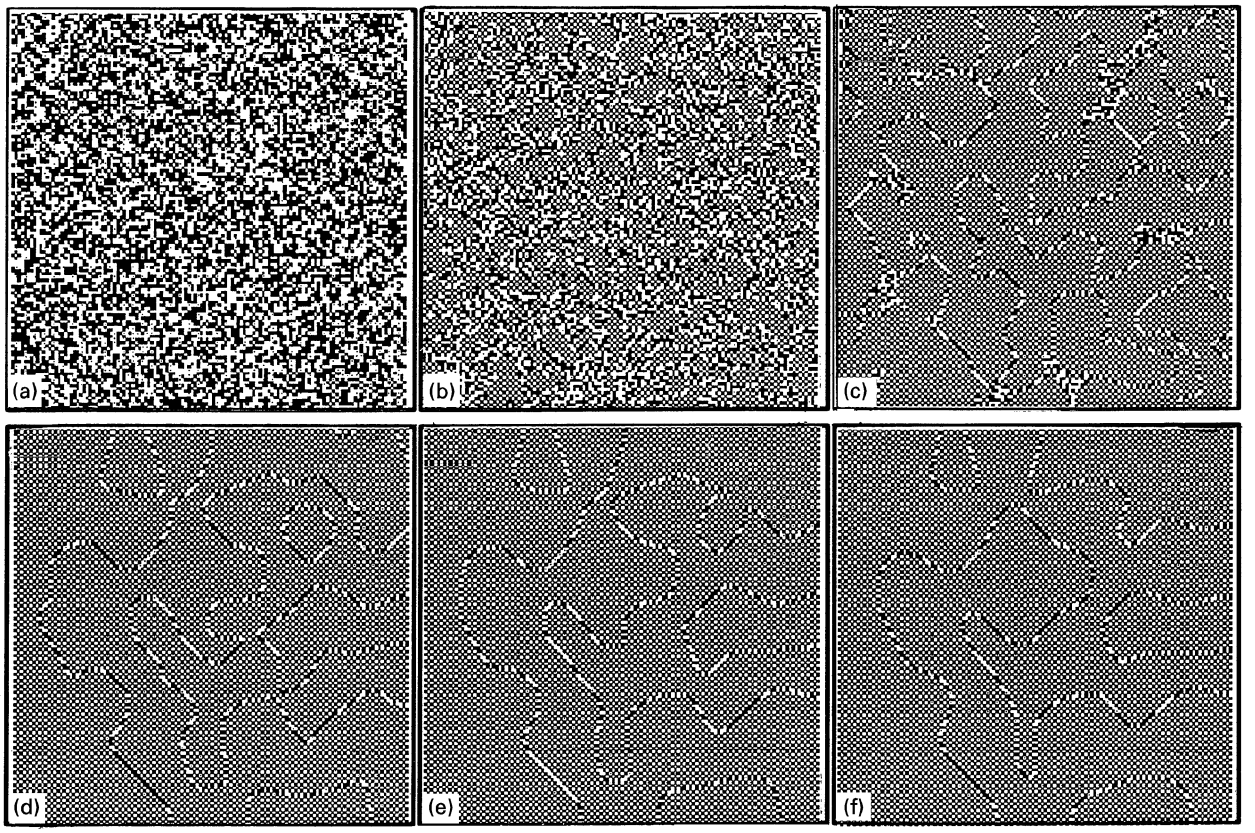

Figure 2 Time development of the ordered domains calculated for a computational cell 256×256, where the initial condition is selected for $n(\mathbf{p})$ to be close to 0 or 1 for each lattice point. (a) $t^* = 0.0$, (b) $t^* = 0.1$, (c) $t^* = 0.3$, (d) $t^* = 1.0$, (e) $t^*1.6$, (*f*) $t^* = 2.5$.

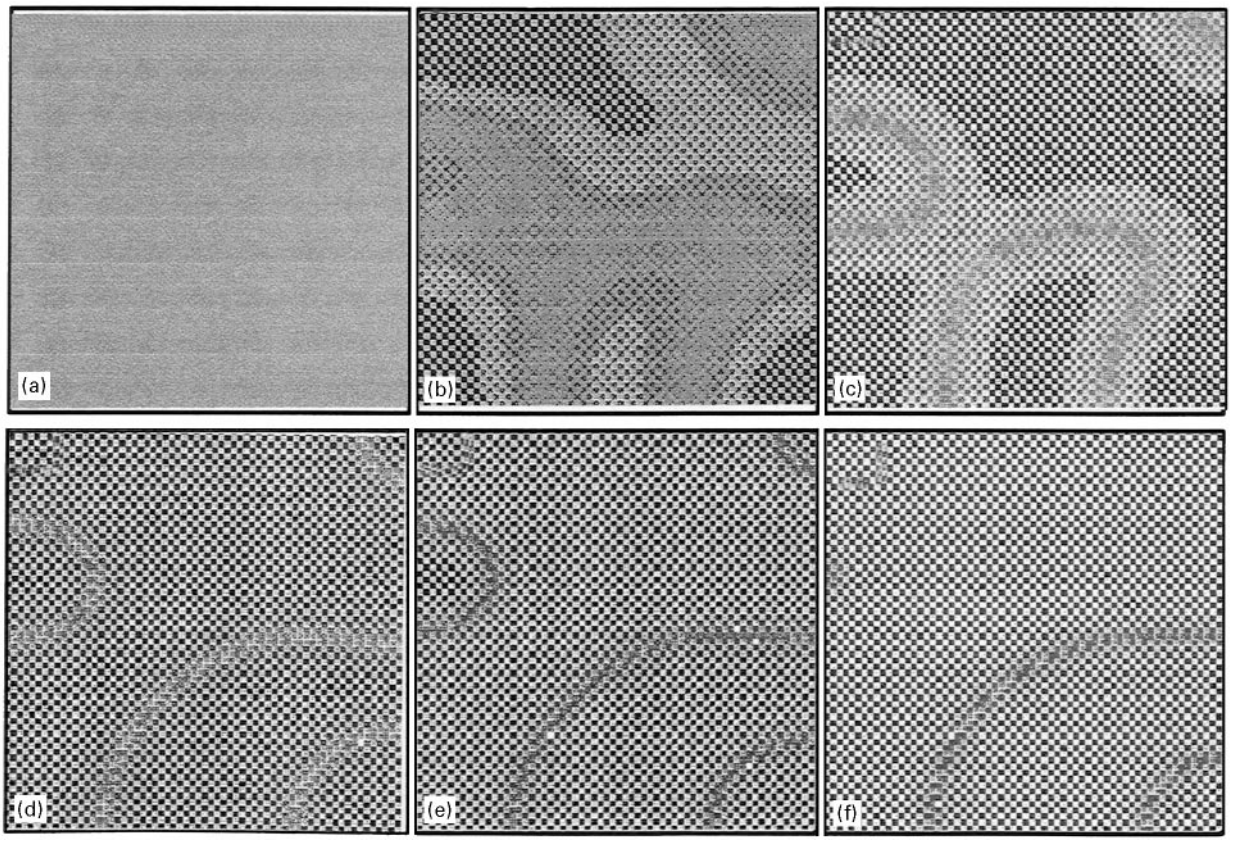

Figure 3 Computer simulations at different compositions at $T^* = 0.2$ for the same ageing time for a computational cell of 128×128; the value of the occupational probabilities $n(\mathbf{p})$ at each lattice site is shown grey areas, with the darkest for $n(\mathbf{p})$ close to 1.0 and the lightest for $n(\mathbf{p})$ close to 0.0. (a) $c = 0.27$, (b) $c = 0.29$, (c) $c = 0.30$, (d) $c = 0.35$, (e) $c = 0.40$, (f) $c = 0.50$.

ordered domains have approximately the same ordered parameter. Subsequently, and for the remain concentrations up to stoichiometry, the same behaviour occurs. Points "e" and "f" in Fig. 3 show the simulation for two points at $c = 0.4$ and the stoichiometry $c = 0.5$, as examples. At this concentration, the only difference is in increasing the area of the large-order domains at the expense of the small ones, which leads to the disappearance of the short APBs.

The morphology generated here shows a good similarity to the experimental transmission electron microscopy (TEM) observation of the ordering system of a binary alloy Fe–Al, which is based upon the macroscopic composition gradient method. In this method, a sample of Fe–50 at % Al was prepared by arc melting. The specimen was melted on a cooled pure iron in the same way. A sample, cut vertically through the Fe/Fe–50 at % Al interface, was aged at 1023 K for a long duration inside an evacuated silica tube. It was then prepared for electron microscopy after the quenching process. Details of this experimental method will be published in a separate paper [23]. Fig. 4 shows a dark-field image of a sample prepared by this method.

As an application of Fig. 3, the long-range order parameter is calculated according to Equation 8 at each lattice site. The result is represented in Fig. 5, which gives an explanation of Fig. 3, and accordingly, the ordering kinetics. Where the value of the LRO parameter, $|\eta|$, is taken as a function of composition for the same ageing time ($t^* = 4.0$), we can divide this figure into four parts. The first part is the disordered area which has zero LRO parameter. The second part begins approximately at the transition line where the LRO parameter just crosses the transition line and increases sharply with a small increase of the concentration (this part represents the beginning of the cooperative phenomenon with the coarsening of the antiphase domains boundary). The third part shows an increase of the LRO parameter but smaller than the second part, and represents the coalescence of the order domains and the contraction of the phase boundaries. The fourth part is where the LRO parameter seems to reach to an equilibrium value, where with increasing concentration, a slight change occurs in the value of the LRO parameter, caused by the movement of the APBs.

For longer ageing times, the same behaviour occurs at $t^* = 20.0$, except for the shift of the starting point of ordering to a somewhat lower concentration.

The LRO parameter is also taken as a function of concentration at different ageing temperatures ($T^* = 0.2$ and $T^* = 0.23$). At $T^* = 0.23$ (Fig. 6) the same behaviour occurs as for the case of $T^* = 0.2$ with some decrease in the value of the LRO parameter.

4.3. The competition of ordering with ageing time

The domain boundaries completely vanish at equilibrium, but it is possible, in some cases, to produce

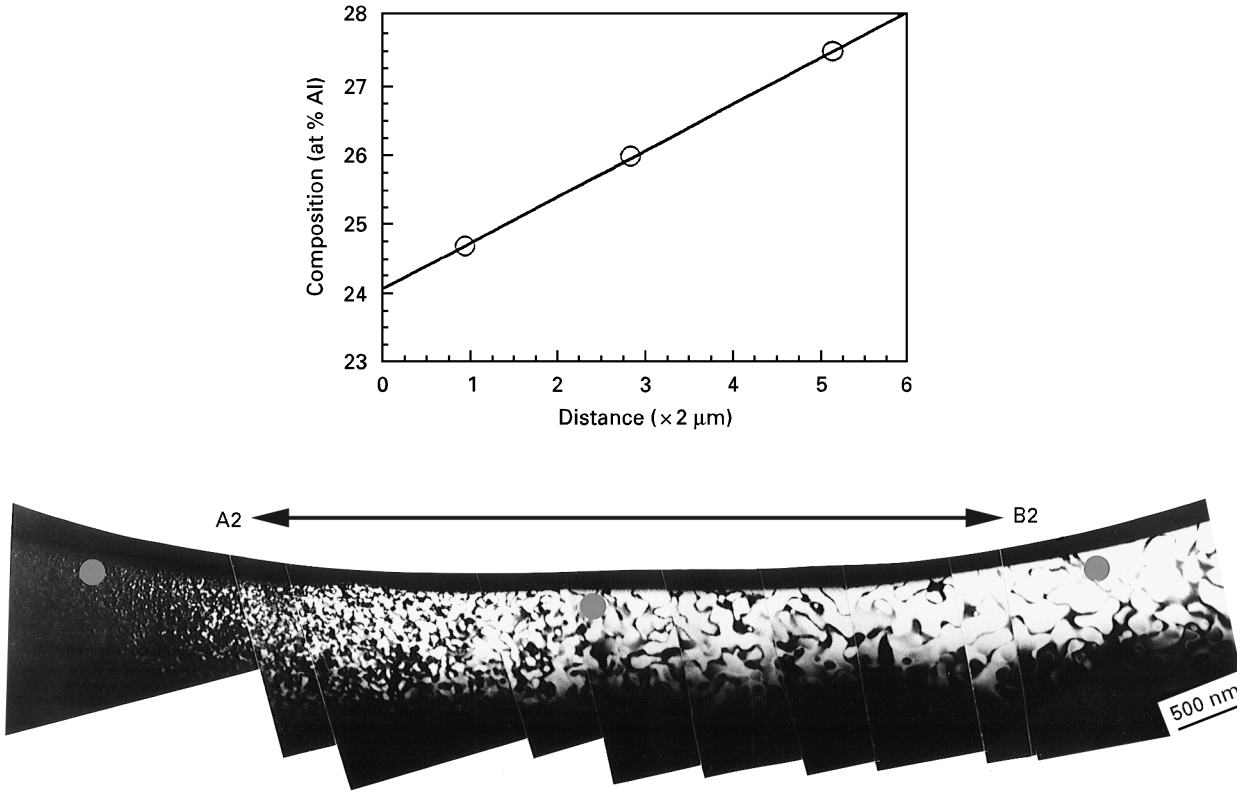

Figure 4 Microstructure of a composition gradient alloy in the Fe–Al system, aged at 1023 K for 86.4 ks.

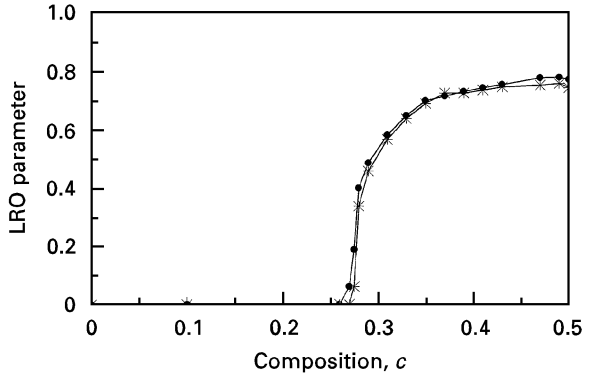

Figure 5 Composition dependence of the LRO parameter at different reduced times for $T^* = 0.2$: (∗) $t^* = 4$, (●) $t^* = 20$.

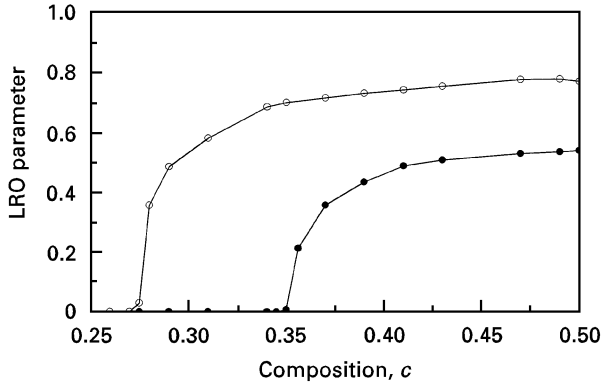

Figure 6 Composition dependence of the equilibrium LRO parameter at different ageing temperatures and the same ageing time: (●) $T^* = 0.23$, (○) $T^* = 0.2$.

a metastable structure in which the domains persist for long periods [20] and the structure of highly ordered antiphase domains is analogous in many ways to a polycrystalline aggregate of strain-free grains.

For a clearer interpretation for the kinetics of ordering, the LRO parameter was developed for two cases, one at a composition near to the transition point and the other at stoichiometry, as a function of ageing time at a reduced temperature, $T^* = 0.2$, for a computational cell of 256×256 lattice sites.

4.3.1. At stoichiometry

Fig. 7 shows the growth of the ordered domain with ageing time. The initial configuration at $t^* = 0.0$ is completely disordered with an occupation probability of $\cong 0.5$ and $|\eta| \approx 0.0$. With increasing the ageing time and at $t^* = 0.6$, the behaviour characteristic of the cooperative phenomenon is seen, characterizing the second-order phase transition (Fig. 7b). As first pointed out by Bragg [24], the superlattice, which has only two types of antiphase domains (e.g. B2 structure), cannot exist as aggregates of small domains. Accordingly, the same type coalescence to form larger domains, which coarsen, and the domain boundary contracts leading to a further reduction of the disordered area and consequently increasing the ordered area. This process is relatively rapid, during which the free energy decreases continually. Thus the co-operative phenomenon occurs, and, consequently, the coalescence of the ordered phase domain and the formation of the antiphase boundary already attained at $t^* = 0.8$ as in Fig. 7c. In Fig. 7d the equilibrium

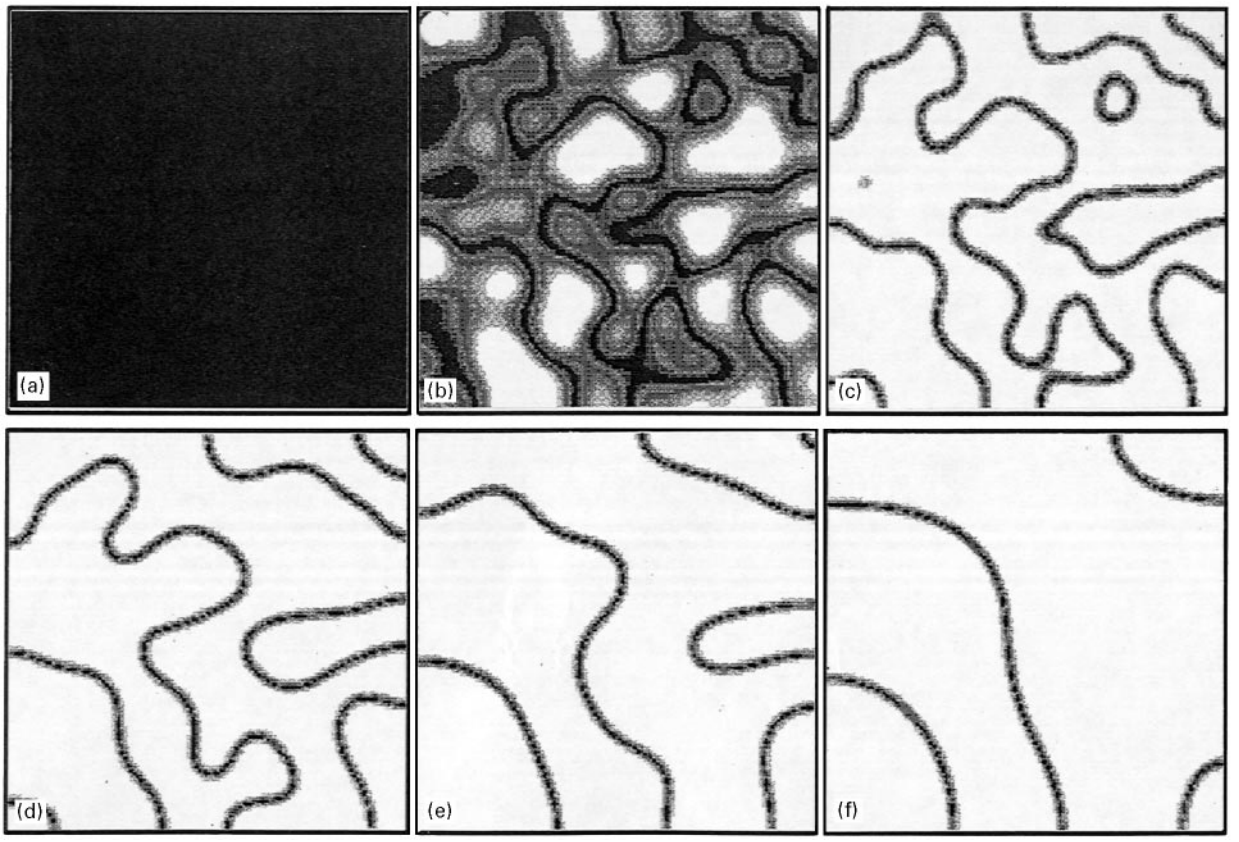

Figure 7 The temporal evolution of the LRO parameter for a computational cell of 256×256 lattice sites, at $c = 0.5$ and $T^* = 0.2$; the value of the LRO parameter (η) at each lattice site is shown by grey areas, with the darkest for η close to 0.0 and the lightest for η close to 0.9. (a) $t^* = 0.0$, (b) $t^* = 0.6$, (c) $t^* = 0.8$, (d) $t^* = 1.4$, (e) $t^* = 4.0$ (f) $t^* = 10.0$.

configuration is seemingly attained, so the structure subsequently changes more slowly and the reduction in the free energy is obtained by movement of the domain boundaries. As a result of this movement, larger domains grow, small ones shrink and each boundary tries to straighten rapidly, so as to give a structure of a few large domains extending right across the crystal, as shown in Fig. 7e and f.

It should be noticed that the LRO parameter is distributed homogeneously all over the ordered domains and that the domains are very close to each other, making the antiphase domain boundary very thin.

4.3.2. Near the transition line ($c = 0.29$)

Fig. 8 shows the evolution of the LRO parameter for $c = 0.29$. Fig. 8a, $t^* = 0.0$, shows a completely random distribution of atoms with LRO parameter $\simeq 0.0$. The order domain begins to appear with a small number after long times compared to the case of stoichiometry. For the second-order phase transition, this is referred to as a critical slowing down phenomenon. The domains have the highest LRO parameter at the centre which decreases gradually to reach zero at the APBs, and is wider than that for the stoichiometry case, see Fig. 8b, $t^* = 2.6$.

Contrary to the case of decomposition, where the LRO parameter annihilate predominantly at the APB [18] causing the congruent ordered domains to contract and the disordered domain to expand, here the LRO parameter relaxes from the centre towards the APBs, leading to the formation of ordered domains, with an approximately stable value at the centre, decreasing gradually to zero at the APB. This relaxation of the LRO parameter causes the ordered domains to become closer, while the APBs are further apart than in the case of stoichiometry (Fig. 8c, $t^* = 3.0$).

At $t^* = 5.0$ (Fig. 8d), the equilibrium state seems to be attained, and the configuration consists of an ordered domain with an LRO parameter with a stable value for an area at the centre, decreasing gradually towards the APBs which did not suffer any change in thickness.

Subsequently, for long ageing times (Fig. 8e and f, $T^* = 10.0$ and 25.0), a simple movement of the APBs causes further reduction of the free energy.

This behaviour is in good agreement with the experimental work of Loiseau *et al.* [15]. They studied the transition between the B2 and DO_3 phases of Fe–Al using transmission electron microscopy through *in situ* heating experiments.

As an application, the value of the LRO parameter as a function of ageing time for two different concentrations, one at stoichiometry and the other close to the transition line, is represented by Fig. 9. This figure clearly shows that the kinetics of ordering at the two different concentrations is quite different in many aspects:

(i) at stoichiometry, ordering occurs at an earlier time than that for values of c close to the transition

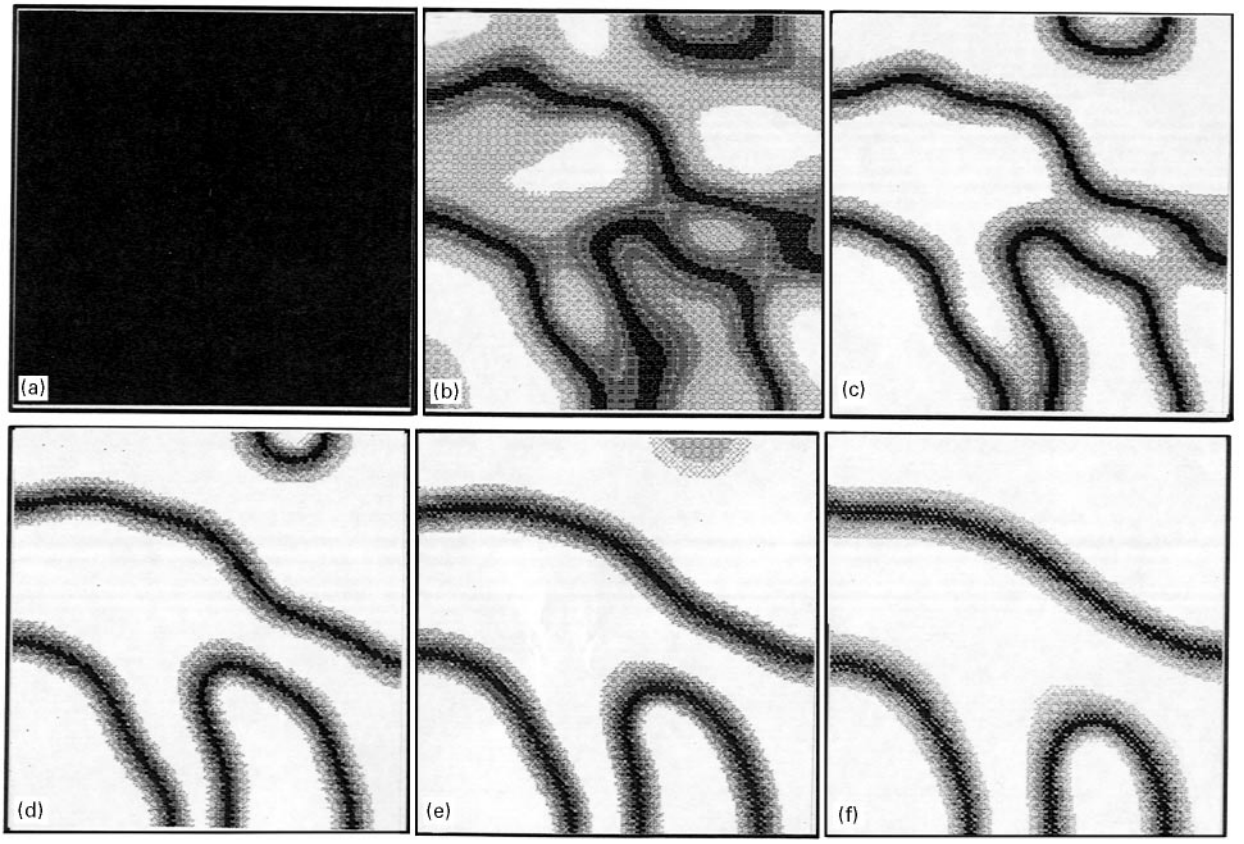

Figure 8 The temporal evolution of the LRO parameter for a computational cell of 256×256 lattice sites, at $c = 0.29$ and $T^* = 0.2$; the value of the LRO parameter (η) at each lattice site is shown by grey areas with the darkest for η close to 0.0 and the lightest for η close to 0.6. (a) $t^* = 0.0$, (b) $t^* = 2.6$, (c) $t^* = 3.0$, (d) $t^* = 5.0$, (e) $t^* = 10.0$ (f) $t^* = 25.0$.

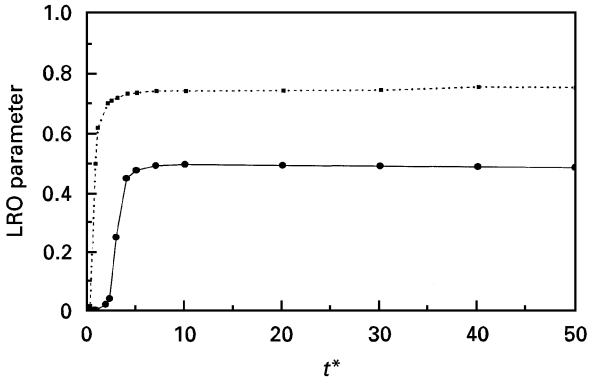

Figure 9 Time dependence of the LRO parameter at different compositions for $T^* = 0.2$: (●) $c = 0.29$, (■) $c = 0.50$.

line. This is the critical slowing down phenomenon which occurs before significant ordering. It was found that for, c close to the transition line, ordering starts at about 2.4 units of reduced time, while it is at only about 0.5 units of time for stoichiometry;

(ii) ordering at stoichiometry occurs between $t^* = 0.5$ and $t^* = 1.0$ while for c close to the transition line it occurs between $t^* = 2.2$ and $t^* = 4.0$; after that, evolution of the occupation probability corresponds to coalescence and coarsening of ordered domains, making the LRO parameter for the two cases approximately stable, with some increase corresponding to the simple movement of the APBs;

(iii) in the stability region, the value of the LRO parameter for values of c close to the transition line is smaller than that for the case of stoichiometry, because the antiphase domain boundary for the first case is somewhat wider than that for stoichiometry, making the ordered domain area near the transition line smaller than that at stoichiometry. In addition, the LRO parameter has a gradient value through the ordered domains for values of c close to the transition line (the small vlaue at the APBs increases on going towards the centre of the ordered domains) while it is approximately the same all over the ordered domains at stoichiometry.

4.4. The competition of ordering with the transition temperature

For the sake of comparison, the long-range order parameter was studied as a function of the transition temperature, where the critical temperature of ordering, T_c^*, is determined at $c = 0.5$ according to the equation

$$T_c^* = \eta \Big/ \left(2\ln\frac{1+\eta}{1-\eta}\right) \tag{12}$$

The plot of the equilibrium LRO parameter as a function of the T/T_c^*, calculated from the mean of the Khachaturyan equation, together with the value calculated according to the Bragg–William approximation and the Bethe approximation [25], is shown in Fig. 10. The LRO parameter at first does not change with increasing temperature, then decreases gradually,

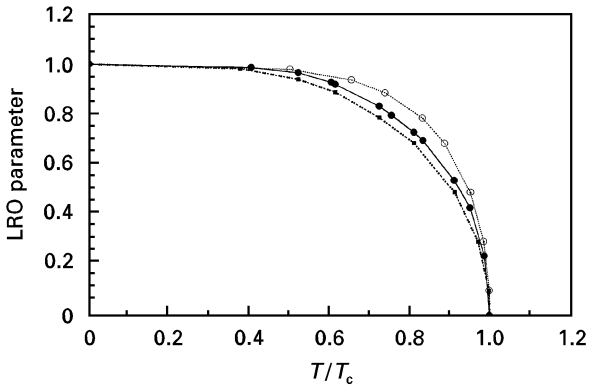

Figure 10 Equilibrium LRO parameter as a function of temperature. (· · – ■ – · ·) Bragg–Williams, (—●—) present calculation, (··· ⊙ ···) Bethe.

but reaches zero more abruptly. Consequently, its complete disappearance is marked by a second type of phase transition, because it is known that the type of transition can be correlated with the abruptness of the disappearance the long-range order parameter. From the figure we can see that Khachaturyan's kinetic model produces a thermodynamic description in between the Bragg–William the Bethe approximations.

We believe that the Khachaturyan-type diffusion equation, albeit with more tedious work to obtain the composition dependency of the kinetic coefficients, can be applied to simulate the ordering of the real alloy system, because the equation has already been successfully applied to the case of phase decomposition inside the spinodal phase [19] for the real alloy system.

5. Conclusions

1. Khachaturyan's diffusion equation can successfully describe the process of ordering for a disordered phase annealed within a single-phase field of an ordered phase in a phase diagram. This process exhibits a behaviour characteristic of a co-operative phenomenon characterizing the second-order phase transformation, going through order domain coalescence, antiphase domain coarsening and finally a simple movement of the APBs.

2. Time development of the long-range order (LRO) parameter, according to the concentration wave formalism at different concentrations for the same temperature or vice versa, describes the kinetics of the ordering. Inside the ordered region, it is interesting to observe that a phenomenon, called the critical slowing down, with further symmetry breakdown, occurs. Near the transition line, the cooperative phenomenon takes some time to appear, followed by a sharp increase of the LRO parameter up to the equilibrium value; on going away from the transition line, the appearance time for the cooperative phenomenon becomes shorter, the increase in the LRO parameter becomes sharper, reaching a larger equilibrium value. Just outside the transition line, inside the disordered region, the LRO parameter vanishes.

3. There is good agreement between these results and the most recent experimental transmission electron microscopy work.

Acknowledgement

The present research was financially supported by a grant-in-aid for Scientific Research from the Ministry of Education, Science and Culture of Japan, for which the authors are very grateful.

References

1. C. TAMMAN, *Z. Anorg. Allg. Chem.* **107** (1919) 1.
2. L. GUTTMAN, *Solid State Phys.* **3** (1956) 145.
3. S. M. ALLEN and J. W. CAHN, *Acta. Metall.* **23** (1975) 1017.
4. H. KUBO and C. M. WAYMAN, *ibid.* **28** (1980) 395.
5. S. V. SEMENOVSKAYA, *Phys. Status Solidi B* **64** (1974) 291.
6. W. A. SOFFA and D. E. LAUGHLIN, *Acta Metall.* **37** (1989) 3019.
7. H. MATSUDA, H. KUROKI and T. EGUCHI, *Trans. Jpn Inst. Metals* **12** (1972) 390.
8. G. H. VINEYARD, *Phys. Rev.* **102** (1956) 981.
9. K. KAWASAKI, *ibid.* **145** (1966) 224.
10. J. D. GUNTON, M. S. MIGUEL and P. S. SAHNI, in "Phase Transformations and Critical Phenomena", edited by J. Leowitz, Vol. 8 (Academic Press, London 1983) p. 267.
11. H. SATO and R. KIKUCHI, *Acta Metall.* **24** (1976) 797.
12. K. GSCHWEND, H. SATO and R. KIKUCHI, *Chem. Phys.* **69** (1978) 5006.
13. B. FULTZ, in "Statics and Dynamics of Alloy Phase Transformations", edited by P. E. A. Turchi and A. Gonis (Plenum Press, New York, 1994) p. 669
14. L. Q. CHEN and J. A. SIMMONS, *Acta Metall. Mater.* **42** (1994) 2943.
15. A. LOISEAU, C. RICOLLEAU, L. POTEZ and F. DUCASTELLE, in "Solid → Solid Phase Transformations", edited by W. C. Johnson, J. M. Howe, D. E. Laughlin and W. A. Soffa (Minerals, Metals and Materials Society, Warrendale, Pennsylvania, 1994) p. 385.
16. A. G. KHACHATURYAN, in "Progress in Materials Science", edited by B. Chalmers, J. W. Christian and T. B. Massalski, Vol. 22 (Pergmon Press, Oxford, England 1978).
17. L. Q. CHEN and A. G. KHACHATURYAN, *Scripta Metall.* **25** (1991) 61.
18. L. Q. CHEN and A. G. KHACHATURYAN, *Acta Metall. Mater.* **39** (1991) 2533.
19. T. KOYAMA, T. MIYAZAKI and A. M. MEBED, *Metall. Mater. Trans. A* **26** (1995) 2617.
20. J. W. CHRISTIAN, "The theory of Transformation in Metals and Alloys", 2nd Edn, Part I (Pergamon Press, Oxford, England 1981) p. 206.
21. L. Q. CHEN and A. G. KHACHATURYAN, *Phys. Rev. Lett.* **70** (1993) 1477.
22. Y. WANG, L. Q. CHEN and A. G. KHACHATURYAN, *Acta Metall. Mater.* **41** (1993) 279.
23. S. KOBAYASHI, T. KOYAMA and T. MIYAZAKI, in "Proceedings of Asian Conference of X-ray and Related Investigations (ACXRI 96)" (Ipoh, Malaysia, 1986) p. 21.
24. W. L. BRAGG, *Proc. Phys. Soc.* **52** (1940) 105.
25. H. YAMAUCHI, Scripta Metall. **7** (1973) 109.

Received 23 February 1996
and accepted 17 April 1997